

RSC Advances



This is an *Accepted Manuscript*, which has been through the Royal Society of Chemistry peer review process and has been accepted for publication.

Accepted Manuscripts are published online shortly after acceptance, before technical editing, formatting and proof reading. Using this free service, authors can make their results available to the community, in citable form, before we publish the edited article. This *Accepted Manuscript* will be replaced by the edited, formatted and paginated article as soon as this is available.

You can find more information about *Accepted Manuscripts* in the [Information for Authors](#).

Please note that technical editing may introduce minor changes to the text and/or graphics, which may alter content. The journal's standard [Terms & Conditions](#) and the [Ethical guidelines](#) still apply. In no event shall the Royal Society of Chemistry be held responsible for any errors or omissions in this *Accepted Manuscript* or any consequences arising from the use of any information it contains.

ARTICLE

Metal ions doped carbon dots with strongly yellow photoluminescence

Cite this: DOI: 10.1039/x0xx00000x

Jian Cheng, Cai-Feng Wang, Yan Zhang, Shengyang Yang, Su Chen *

Received 00th January 2012,
Accepted 00th January 2012

DOI: 10.1039/x0xx00000x

www.rsc.org/

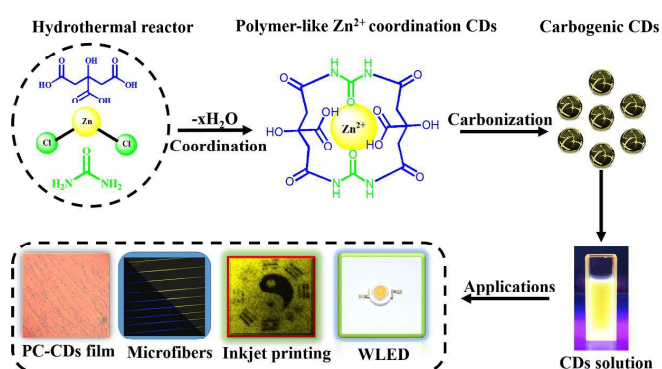
We demonstrated a simple strategy for facile generation of robust yellow photoluminescence (PL) carbon dots (CDs), along with 51.2% quantum yield (QY) via metal ions doped method for the first time. These as-synthesized CDs were carried out using zinc ions and citric acid as the precursor via one-pot solvothermal method, producing excitation-independent zinc ions doped CDs, which may be the highest reported QY on the yellow PL emission CDs. Then, we thoroughly discussed the formation mechanism of high property CDs, which is attributed to the radiative recombination of electrons and holes trapped on the CDs surface. For more practice, various types of applications by using as-prepared CDs have been done, such as bifunctional photonic crystal film, fluorescent microfiber and patterns.

Introduction

Carbon dots (CDs) have sparked tremendous interest due to their splendid and novel properties, such as bright fluorescence, high photostability, low toxicity, excellent biocompatibility.¹⁻³ Currently, many approaches have been developed involving pyrolysis,⁴ chemical oxidation,⁵ laser ablation,⁶ microwave-assisted synthesis,⁷ plasma treatment⁸ and hydrothermal synthesis methods,⁹ which are applied in various applications, such as bioimaging, photovoltaic devices and biosensor applications.¹⁰⁻¹² Although much progress toward CDs has been made, the quantum yield (QY) of previously reported CDs is however not high with only a few exceptions. Another indication is, in most case, the reported emission colors of CDs are usually dull blue, thus limiting their further extensive application. To solve it, much effort focused on non-metallic organic and inorganic metals doped-CDs, along with higher QY and full-color CDs. In this respect, Dong et al. used CDs co-doped with nitrogen and sulfur to effectively increase their QY.¹³ Zhang et al. synthesized carbon dots with tunable luminescence by N doping.¹⁴ Sun's group realized green luminescence CDs with high QY by doping inorganic salt (C_{ZnS}-dots and C_{TiO2}-dots).¹⁵ In spite of some CDs with multi-color under the same excitation wavelength have been reported.^{16, 17} The breakthrough in photoluminescence (PL) quantum yield (QY) and multi-color PL emission CDs under the same excitation wavelength, especially yellow PL emission is therefore highly expected.

Herein, we demonstrated a simple strategy for facile generation of robust yellow photoluminescence CDs, along with 51.2% QY via metal ions doped method for the first time. These as-synthesized CDs were carried out using zinc ions and citric acid

as the precursor via one-pot solvothermal method, producing excitation-independent zinc ions doped CDs (noted as Zn²⁺-doped CDs), which may be the highest reported QY on the yellow PL emission CDs. Then, we thoroughly discussed the formation mechanism of as-synthesized CDs, which is attributed to the radiative recombination of electrons and holes trapped on the CDs surface. For more practice, we utilized these strongly yellow PL Zn²⁺-doped CDs coupling with poly (styrene-*co*-methacrylic acid) (PS-*co*-PMAA) mono-dispersed colloid to create a photonic crystal film (PC-CDs) with bifunction (visible light optical and photoluminescence dual properties) by vertical deposition method. Beside the as-prepared Zn²⁺-doped CDs could be also good candidate for applications in inkjet printing pattern and LED field. This strategy is simple, and would continue to create other robust carbon dots, which allows CDs to extensive promising applications.



Scheme 1 Synthetic route schematic model: using citric acid, urea and zinc chloride. From ionization to coordination, condensation to polymerization, carbonization and their applications in fluorescent hybrid materials.

Results and discussion

The synthetic procedure of Zn²⁺-doped CDs involved dehydration, coordination and carbonization three stages (seen in Scheme 1). Initially, the coordination action between carbonyl, carboxyl groups and Zn²⁺ (0.1 mmol Zn²⁺ in 10 mL toluene) derived from the precursor occurred after dehydration stage.¹⁸ Then, the coordinated compound underwent a continuous dehydration process to form polymer-like CDs, which were further carbonized to form the Zn²⁺-doped CDs along with prolonging reaction time under the high temperature.⁶ We followed to apply the as-synthesized Zn²⁺-doped CDs with robust bright yellow PL intensity to various applications.

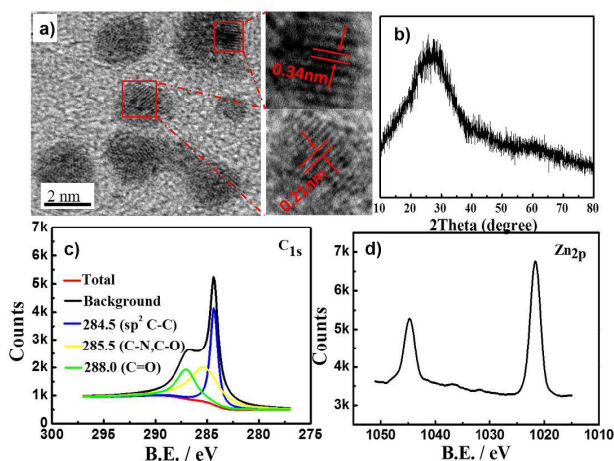


Fig. 1 (a) HRTEM images of the Zn²⁺-doped CDs. Typical single CDs with lattice parameters of 0.34 nm and 0.21 nm, respectively. (b) XRD pattern. XPS spectra of the Zn²⁺-doped CDs. (c) High-resolution C_{1s}, (d) Zn_{2p} peaks of the Zn²⁺-doped CDs.

The morphology of Zn²⁺-doped CDs were confirmed by transmission electron microscopy (TEM) analyses. Fig. S1a, ESI† shows TEM images of the Zn²⁺-doped CDs, revealing the as-synthesized Zn²⁺-doped CDs are uniform dispersion without apparent aggregation and particle diameters of 2-5 nm (Fig. S1b, ESI†). From the high-resolution TEM (HRTEM) images we can distinctly see lattice of the Zn²⁺-doped CDs. Fig. 1a shows the lattice spacing of 0.34 nm should be the spacing between graphene layers (002 facet), while the lattice spacing of 0.21 nm agrees with that of in-plane lattice spacing of graphene (100 facet). This result is similar to those of many other reported CDs.^{19, 20} The XRD patterns of the Zn²⁺-doped CDs (Fig. 1b) displays a peak centered at 25.5° (0.34 nm),¹³ which is ascribed to disordered carbon atoms, similar to the graphite lattice spacing.

The atomic force microscopy (AFM) image (Fig. S2a, ESI†) shows the landform height of the as-synthesized Zn²⁺-doped CDs, with the range from 2.5 to 4.5 nm (Fig. S2b, ESI†). X-ray

photoelectron spectroscopy (XPS) results indicate the Zn²⁺-doped CDs are mainly composed of carbon, nitrogen, oxygen and zinc. Also, the high resolution XPS spectrum of C_{1s} exhibits (sp² C-C), (C-O, C-N), (C=O) main peaks at corresponding binding energy of 284.5 eV, 285.5 eV and 288.0 eV (Fig. 1c). Fig. 1d shows the XPS spectrum of Zn_{2p} peaks noted at 1045 eV, 1023 eV, respectively. The thermogravimetric analysis (TGA) result indicates there exists 10% zinc oxide compound in Zn²⁺-doped CDs when the decomposition temperature is higher than 580°C (Fig. S3a, ESI†). The above results also confirm the zinc ions have already been doped onto CDs.

We further characterized Zn²⁺-doped CDs by the Fourier Transform Infrared (FTIR) and Microscopic Fourier Transform Infrared (MFTIR) spectra (Seen in Fig. S3b, Fig. S4, ESI†). The peaks noted at 3430 cm⁻¹, 1650 cm⁻¹ and 1120 cm⁻¹ are ascribed to characteristic peaks of hydroxyl group (-OH) and carbonyl group (C=O), asymmetric stretching vibrations of C-N, respectively. Strong intensity of the Zn-O band at near 700 cm⁻¹ and 450 cm⁻¹ imply that complexation took place by metal-oxygen binding. While we also observed carboxylic acid spectra with a main symmetric ν_s (COO⁻) band around 1450cm⁻¹ and asymmetric ν_{as} (COO⁻) band around 1650cm⁻¹.²¹ By contrast FTIR results of Zn²⁺-doped CDs sample with control sample (without Zn²⁺-doped), we can obviously observe the intensities of characteristic peaks noted at 3430 cm⁻¹ (-OH) and 1650 cm⁻¹ (C=O) are decreased. (Fig. S3b, ESI†), together with the MFTIR evidence shows that red color area intensity (represented the intensity of characteristic peak) noticed at 3430 cm⁻¹ (-OH) and 1650 cm⁻¹ (C=O) can be transferred or decreased to partially yellow color area (Fig. S4, ESI†). It is clear that the asymmetric carboxylate vibrations of the control sample appear at higher frequencies than the Zn²⁺-doped CDs sample. It can be associated with a stronger interaction of carboxylic acid with the zinc sites. Carboxylate ions can coordinate in several ways, including unidentate ligand, chelating ligand and bridging bidentate ligand configurations. Since each coordination has a specific ν_{as} (COO⁻) and ν_s (COO⁻) peak position, the peak separation (Δν (COO⁻) = (ν_{as} (COO⁻) - ν_s (COO⁻))) can be used to understand the coordination type of the carboxylates. According to peak separation (Δν (COO⁻) > 160 cm⁻¹) and metal-oxygen binding (Zn-O), the plausible complex structure for Carboxylate ions and Zn²⁺ product is proposed as chelating ligand.^{22, 23}

Fig.2 shows a series of optical characterization of as-prepared CDs. The product, Zn²⁺-doped CDs, has high fluorescence and a bright yellow color under UV lamp at a very low concentration (0.1 mg.mL⁻¹). There exists a sharp absorption peak of UV/Vis spectrum centered at 460 nm as well as we can observe a narrow distribution PL peak with high PL intensity noted at the emission wavelength of 580 nm (λ_{ex}=380 nm) in Fig. 2a. The QY of the as-obtained Zn²⁺-doped CDs is as high as 51.2% using Rhodamine 6G in ethanol as a standard (see details in the ESI†). To the best of our knowledge, this is the highest QY value of CDs on yellow PL in previously reported literatures, whereas an example reported the highest QY of CDs with yellow PL only reach 12%.²⁴ Another indication is that

Zn²⁺-doped CDs do not have PL excitation-dependence, which is the common property for other traditional CDs (Fig. 2b). Interestingly, the PL intensity of emission in this case, is increased with the decrease of excitation wavelength, which is undiscovered previously. It is highly associated with zinc doping behaviour. We further investigated PL properties and fluorescence decay behaviours of two samples, Zn²⁺-doped CDs and control CDs, shown in Fig. 2c and 2d, respectively. Under the same tested condition, there exists an obvious red-shift occurrence of the PL peak when comparing Zn²⁺-doped CDs sample with control sample (Fig. 2c). Also, there is clearly tailing phenomenon of control sample in PL curve, which occurs in most reported CDs. However, this tailing phenomenon is well resolved by the method of zinc ions doping with CDs. The symmetry of the PL peak on Zn²⁺-doped CDs is significantly improved, which means their particles size is more uniform. Furthermore, fluorescence decays of Zn²⁺-doped CDs and control CDs were measured by using the time-correlated single photon counting (TCSPC) technique (Fig. 2d). We calculated the average lifetime (τ) of Zn²⁺-doped CDs and control CDs as 6.8 ± 0.05 ns and 5.5 ± 0.05 ns, respectively ($\chi^2 < 1.1$) (See details in the ESI[†]). The Zn²⁺-doped CDs average lifetime is longer than that of control CDs. Mechanistically, the longer lifetime of carbon-based photoluminescence has been attributed to passivated defects (passivated by organic or inorganic via either covalent linkages or chemical adsorption) on the CDs surface acting as excitation energy traps.²⁶ More specifically, due to the zinc ions doped on the CDs, the CDs surface have been passivated, which exhibit longer lifetime than that of control CDs. That is, the Zn²⁺-doped CDs have more PL stability.

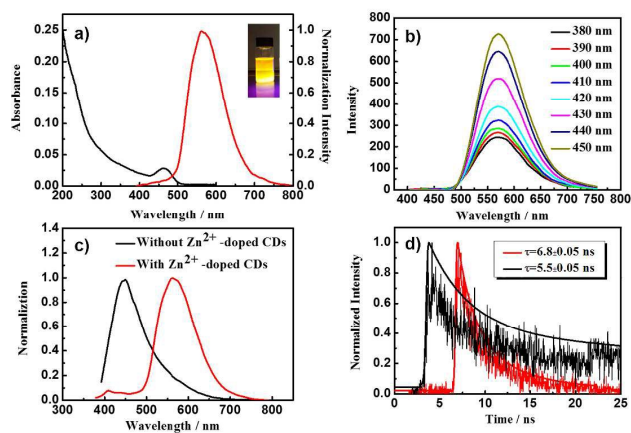


Fig. 2 a) Absorption (ABS) and fluorescence (FLSC, 380 nm excitation) spectra of the Zn²⁺-doped CDs. Inset: Photograph of the obtained Zn²⁺-doped CDs under illumination of UV (365 nm) light. b) PL emission spectra of Zn²⁺-doped CDs under different wavelength excitations. c) PL emission spectra of Zn²⁺-doped CDs (red) and without Zn²⁺-doped CDs (black). d) Fluorescence decays of the Zn²⁺-doped CDs (red) and without Zn²⁺-doped CDs (black).

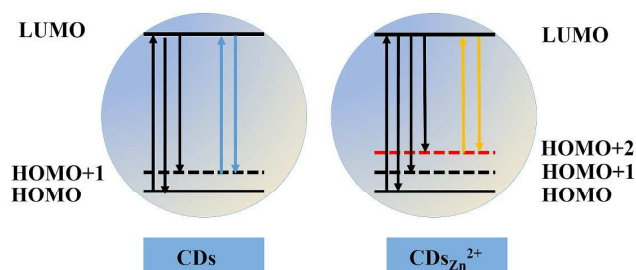


Fig. 3. Schematic illustration of proposed energy levels and electron transition graphic of without Zn²⁺-doped CDs (left) and Zn²⁺-doped CDs (right).

In terms of the reported mechanism, two popular hypotheses, namely electronic conjugate structures²⁵ and emissive traps²⁶ have been proposed. Herein, we inferred that the strong yellow PL emission of the Zn²⁺-doped CDs mainly results from the CD surface passivation doped with zinc ions. Similar result was already reported by Sun group¹⁵, that the strengthened PL of the semiconductor-doped CDs may be rationalized in terms of improved surface passivation by a combination of inorganic surface-doping and organic functionalization. In fact, the PL emissions in CDs are attributed to radiative recombination of the CDs surface-trapped electrons and holes. Hence, it is reasonable that more new energy levels occurred due to zinc ions addition, producing more diverse surface sites and occurrence of PL red-shift.

Then the energy level diagrams of the CDs and Zn²⁺-doped CDs are proposed as illustrated in Fig. 3, and we proposed that Zn²⁺-doped CDs feature similar to those of CDs, and their full-color emissions are mainly derived from different surface states. For the Zn²⁺-doped CDs, besides the HOMO and HOMO+1 energy levels, a new HOMO+2 energy level is introduced after Zn²⁺ doping. Hence, electrons transitions can happen from the new HOMO+2 to LUMO and then the excited electrons can be deactivated by radiative recombination at the same time. This could cause the PL emission in the yellow regions. However, for the control CDs, due to no energy level introduced, which can only induce blue fluorescence as their electrons transitions happen from the HOMO+1 to LUMO. The excited electrons generated by absorption of short wavelength light (HOMO to LUMO) can relax to the HOMO+1 and HOMO+2 through radiative recombination that result in the excitation-independent and broad emission.

The second set of experiments was focused on fabrication of PC film loaded with fluorescent quantum dots (QDs). Up to now, semiconductor QDs have been applied to couple them with colloidal crystals either by *in-suit* growth methods or by electrostatic fixation on the surface of the polymer spheres.²⁷ However, in most cases, the *in-suit* growth methods do not obtain high quality (PL and QY) QDs. The interaction force of electrostatic fixation between QDs and colloidal crystals is usually weak thus leads to ease phase separation. To make the best use of good coordination of this as-prepared Zn²⁺-doped CDs, we employed monodisperse colloidal photonic crystals PS-*co*-PMAA spheres (average size 250 nm, Fig. 4c) combining Zn²⁺-doped CDs to create bifunctional film with PC

structure color and brightly yellow PL dual properties (Fig. 4a and 4b) by vertical deposition method for the first time. Under UV lamp, the film can be changed from red color to be bright yellow fluorescent color. More importantly, brightly yellow PL and non-fluorescent we can clear distinguish when contrasted the Zn^{2+} -doped CDs with without Zn^{2+} -doped CDs composited photonic crystal film (Fig. S5, ESI†). Fig. 4d shows the reflection spectra of PC film and PC-CDs film. A redshift of wavelength but decrease of intensity of the reflection spectrum can be obviously noticed, which might be caused by the changed band structure of PCs. This could be explained by coordination effect between the Zn^{2+} -doped CDs and PS-co-PMAA colloidal crystals containing carboxyl groups. This interaction between them allows the Zn^{2+} -doped CDs to firmly binding to the colloidal crystals, forming uniform fluorescent film, which has tremendous potential applications on sensor and anti-fake field.

In practice, it is desirable that the high QY Zn^{2+} -doped CDs product could be made best of to create white light emitting diode (WLED). Indeed, there are several reports covered that CDs can make WLED.²⁸ However, in most cases the QYs of CDs applied in WLEDs are fairly low, along with dull blue color, limiting their applications. Herein, we employed the yellow PL Zn^{2+} -doped CDs to make a WLED with Commission International d'Eclairage (CIE) coordinates of (0.36, 0.34) (Fig. 4). The result indicates that the Zn^{2+} -doped CDs with robust yellow PL emission can act as the phosphor materials for achieving high performance WLED. On the other hand, we further tried to make use of high QY Zn^{2+} -doped CDs solution as dye ink to construct fluorescent pattern via inkjet printing (Fig. S6, ESI†).¹¹ As expect, the pattern has bright yellow color with "panda" picture under UV light. Also, we fabricated one-dimensional fluorescent microfiber arrays via microfluidic technology. (Fig. S6, ESI†).

h) Luminescence spectra of the blue LED with and without Zn^{2+} -doped CDs coating.

Experimental

Materials

Citric acid monohydrate (CA), urea, zinc chloride (ZnCl_2), toluene, styrene (St), methacrylic acid (MAA), potassium persulfate (KPS) were purchased from Sinopharm Chemical Reagent Co., Ltd. (Shanghai, China). Styrene, methacrylic acid, potassium persulfate were purified before used. Polyvinylpyrrolidone (PVP), rhodamine 6G purchased from Aladdin Chemistry Co., Ltd. Carbon-coated copper grids were supplied by Electron Microscopy Sciences; High-purity water with the resistivity of greater than $18 \text{ M}\Omega\cdot\text{cm}$ was used in the experiments.

Characterizations

High-resolution transmission electron microscope (HRTEM) observation was performed with a Tecnai G2 F30 S-TWIN transmission electron microscope. The element analyses were measured on an Elementar Vario EL cube (Germany). Fourier transform infrared (FT-IR) spectra were recorded on a Nicolet 6700 FT-IR spectrometer. X-ray diffraction (XRD) was performed on a Rigaku Corporation D/max-rC rotating anode X-ray powder diffractometer using a copper target. X-ray photoelectron spectroscopy (XPS) spectra of the Zn^{2+} -doped CDs were performed on an ES-CAIAB250 XPS system with $\text{Al/K } \alpha$ as the source, and the energystep size was set as 0.100 eV. Ultraviolet-visible (UV-vis) absorption spectra were taken with a Perkin-Elmer Lambda 850 UV-vis spectrometer. Photoluminescence (PL) measurements were carried out on a Varian Cary Eclipse spectrophotometer. Time-correlated single-photon counting (TCSPC) data were performed on an Edinburgh FL 900 photocounting system. Thermogravimetric analysis (TGA) measurements were performed on a TA Instruments Q500 TGA analyzer. Atomic force microscopy (AFM) analysis was carried out in the acoustic AC mode on a Molecular Imaging PicoPlus AFM system equipped with a multipurpose scanner and a NanoWorld Pointprobe NCH sensor. Microfluidic spinning microfibers were also observed by an inverted fluorescence microscope (SFM-30I, Shanghai).

Preparation of Zn^{2+} -doped CDs and control CDs.

The reaction was conducted by dissolving citric acid (1 mmol), urea (2 mmol) and ZnCl_2 (1 mmol) in toluene (10 mL) with stirring. These formed a transparent solution with ZnCl_2 disperse in. This suspension was then transferred to a Teflon-line autoclave chamber (25 ml). After that the chamber was sealed and heated at 200°C for 12 h. After the above reaction, the reactor was cooled down to room temperature naturally. The obtained brown solution was centrifuged at 12000 rpm for 20 min to remove large particles and the supernatant were collected. The solid samples can be obtained by evaporating the solvents, and the Zn^{2+} -doped CDs have excellent solubility in

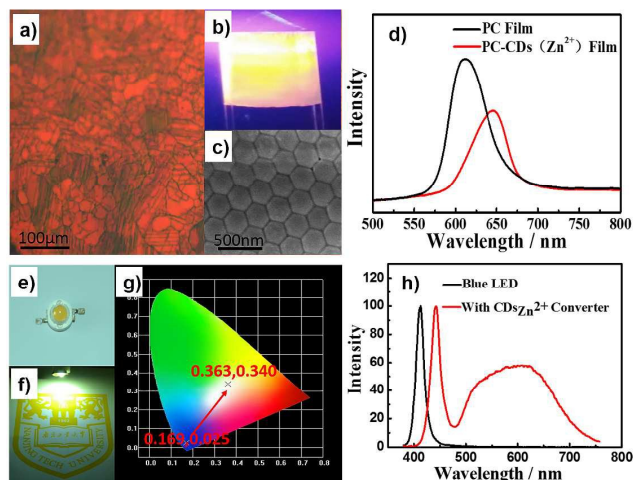


Fig. 4. a) Structural color of PC-CDs $_{\text{Zn}^{2+}}$ film by the Metallurgical Microscopy. b) PC-CDs $_{\text{Zn}^{2+}}$ film under UV-light. c) SEM image of PC-CDs $_{\text{Zn}^{2+}}$ film. d) Reflection spectrum of PC film (black) and PC-CDs $_{\text{Zn}^{2+}}$ film (red). e, f) Photographs of the Zn^{2+} -doped CDs coated LED and applied voltage. g) The CIE chromaticity coordinates for the illuminating blue LED with and without Zn^{2+} -doped CDs layer.

many polar organic solvents or water. Without Zn²⁺-doped CDs synthesis process is the same except for adding ZnCl₂.

Synthesis of PS-co-PMAA photonic crystal

1.3 g of MAA was dissolved in 470 g of purified water in a 1 L round flask, and the stirring speed was set at 300 rpm. After the solution was heated at 98 °C, 20 g St was added and emulsified for 20 min. The polymerization was initiated by 30 g aqueous solution containing 0.75 g KPS and polymerization was allowed to continually for 4 h at 98 °C. After the mixture was quenched with air, the end product was obtained.

Synthesis of PC-CDs film

PC-CDs film was synthesized by combining photonic crystal and CDs through vertical deposition method. 2 mL without Zn²⁺-doped CDs and Zn²⁺-doped CDs (1 mg·mL⁻¹) were added into two parts of 50 mL (0.2 % solid content) as-prepared PS-co-PMAA photonic crystal solution, respectively, and then inserted a glass (clean by piranha solution) into these solutions. Finally putting them into temperature humidity chamber (temperature: 80 °C, humidity: 60) for 24 h.

Preparation of WLED

The ultraviolet InGaN LED chips were used and attached to the bottom of the LED bases. Afterwards, the silicone was mixed with the CDs solution (1 mg CDs in 1 mL toluene) and mixed uniform by stirred. Then put it into a vacuum chamber to remove bubbles. About 30 μL mixture was dispensed into the cup-shaped blank on the LED chip and thermally cured at 120 °C for 1 h. Finally, the optical lenses were fixed on the bottom of the LED chip and the caverns were filled with the silicone. The LED were then further thermally cured at 120 °C for 1h. All the optical performances were detected using ZWL-600 instrument with integral sphere.

Preparation of fluorescent microfibers by microfluidic spinning

3 g PVP was dissolved in 10 g ethanol solution of CDs (0.1 g Zn²⁺-doped CDs or without Zn²⁺-doped CDs) to prepare gel solution at ambient temperature. After well mechanically stirring and ultrasonic to remove bubbles, a homogeneous gel solution was obtained. This as-prepared gel solution was used to make fluorescent microfibers by microfluidic spinning.

Inkjet printing of CDs solution

The solution of CDs (0.1 g Zn²⁺-doped CDs or without Zn²⁺-doped CDs in 10 g ethanol) was printed using a Dimatix DMP 2831 printer, a fluorescent image of blue and yellow patterns were formed on the paper under UV light.

Conclusions

In summary, we have described a convenient and versatile method for fabrication of robust carbon dots with strongly yellow photoluminescence by doping with zinc ions. The method is simple and versatile, various types of doping actions

could be carried out in seeking new kinds of CDs. The product, Zn²⁺-doped carbon dots, has excitation-independence, highly bright yellow photoluminescence with the highest quantum yield of 51.2%. By the first time, we have created the bifunctional film using colloidal PS-co-PMAA microspheres and Zn²⁺-doped CDs, allowing it to have PC structure color and brightly yellow PL dual properties. Some examples for inkjet printing and microfluidic spinning of the as-prepared CDs suggest that the CDs might have a number of applications in anti-fake and sensor field.

Acknowledgements

This work was supported by National Natural Science Foundation of China (21076103, 21474052 and 21176122), Priority Academic Program Development of Jiangsu Higher Education Institutions (PAPD), and Qing Lan Project.

Notes and references

State Key Laboratory of Materials-Oriented Chemical Engineering and College of Chemistry and Chemical Engineering, NanjingTech University (former Nanjing University of Technology), 5 Xin Mofan Road, Nanjing 210009, P. R. China.

E-mail: chensu@njtech.edu.cn

† Footnotes should appear here. These might include comments relevant to but not central to the matter under discussion, limited experimental and spectral data, and crystallographic data.

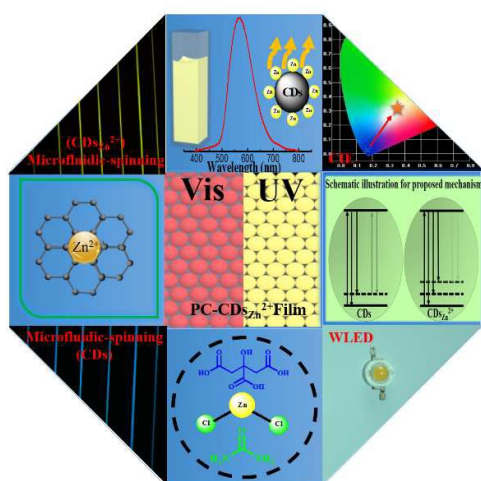
Electronic Supplementary Information (ESI) available: [details of any supplementary information available should be included here]. See DOI: 10.1039/b000000x/

- P. G. Luo, S. Sahu, S.-T. Yang, S. K. Sonkar, J. Wang, H. Wang, G. E. LeCroy, L. Cao and Y.-P. Sun, *J. Mater. Chem. B*, 2013, **1**, 2116.
- L. Cao, S. T. Yang, X. Wang, P. G. Luo, J. H. Liu, S. Sahu, Y. Liu and Y. P. Sun, *Theranostics*, 2012, **2**, 295-301.
- S. Qu, X. Wang, Q. Lu, X. Liu and L. Wang, *Angew. Chem., Int. Ed.*, 2012, **51**, 12215-12218.
- D. Y. Pan, L. Guo, J. C. Zhang, C. Xi, Q. Xue, H. Huang, J. H. Li, Z. W. Zhang, W. J. Yu, Z. W. Chen, Z. Li and M. H. Wu, *J. Mater. Chem.*, 2012, **22**, 3314-3318.
- Z. A. Qiao, Y. Wang, Y. Gao, H. Li, T. Dai, Y. Liu and Q. Huo, *Chem. Commun.*, 2010, **46**, 8812-8814.
- S. T. Yang, X. Wang, H. Wang, F. Lu, P. G. Luo, L. Cao, M. J. Mezziani, J. H. Liu, Y. Liu, M. Chen, Y. Huang and Y. P. Sun, *J. Phys. Chem. C*, 2009, **113**, 18110-18114.
- Q. Wang, X. Liu, L. Zhang and Y. Lv, *The Analyst*, 2012, **137**, 5392-5397.
- J. Wang, C. F. Wang and S. Chen, *Angew. Chem., Int. Ed.*, 2012, **51**, 9297-9301.
- D. Pan, J. Zhang, Z. Li and M. Wu, *Adv. Mater.*, 2010, **22**, 734-738.
- Y. Dong, H. Pang, H. B. Yang, C. Guo, J. Shao, Y. Chi, C. M. Li and T. Yu, *Angew. Chem., Int. Ed.*, 2013, **52**, 7800-7804.
- Y.-Q. Zhang, D.-K. Ma, Y. Zhuang, X. Zhang, W. Chen, L.-L. Hong, Q.-X. Yan, K. Yu and S.-M. Huang, *J. Mater. Chem.*, 2012, **22**, 16714.
- P. Anilkumar, X. Wang, L. Cao, S. Sahu, J. H. Liu, P. Wang, K. Korch, K. N. Tackett, 2nd, A. Parenzan and Y. P. Sun, *Nanoscale*, 2011, **3**, 2023-2027.
- J. Shen, Y. Zhu, X. Yang and C. Li, *Chem. Commun.*, 2012, **48**, 3686-3699.

- 14 C. Fowley, B. McCaughan, A. Devlin, I. Yildiz, F. M. Raymo and J. F. Callan, *Chem. Commun.*, 2012, **48**, 9361-9363.
- 15 S. Zhu, Q. Meng, L. Wang, J. Zhang, Y. Song, H. Jin, K. Zhang, H. Sun, H. Wang and B. Yang, *Angew. Chem., Int. Ed.*, 2013, **52**, 3953-3957.
- 16 W. Wei, C. Xu, L. Wu, J. Wang, J. Ren and X. Qu, *Scientific reports*, 2014, **4**, 3564.
- 17 H. Li, X. He, Z. Kang, H. Huang, Y. Liu, J. Liu, S. Lian, C. H. Tsang, X. Yang and S. T. Lee, *Angew. Chem., Int. Ed.*, 2010, **49**, 4430-4434.
- 18 A. G. Daniel and N. P. Farrell, *Metallomics*, 2014, **6**, 2230-2241.
- 19 X. Wang, K. Qu, B. Xu, J. Ren and X. Qu, *J. Mate. Chem.*, 2011, **21**, 2445.
- 20 Y. Yang, J. Cui, M. Zheng, C. Hu, S. Tan, Y. Xiao, Q. Yang and Y. Liu, *Chem. Commun.*, 2012, **48**, 380-382.
- 21 C. Zhu, J. Zhai and S. Dong, *Chem. Commun.*, 2012, **48**, 9367-9369.
- 22 J. J. Zhang, W. Yang, J. P. Piquemal and P. Y. Ren, *J. Chem. Theory. Comput.*, 2012, **8**, 1314-1324.
- 23 P. Taheri, J. Wielant, T. Hauffman, J. R. Flores, F. Hannour, J. H. W. de Wit, J. M. C. Mol and H. Terryn, *Electrochim. Acta*, 2011, **56**, 1904-1911.
- 24 S. K. Bhunia, A. Saha, A. R. Maity, S. C. Ray and N. R. Jana, *Scientific reports*, 2013, **3**, 1473.
- 25 H. Nie, M. Li, Q. Li, S. Liang, Y. Tan, L. Sheng, W. Shi and S. X.-A. Zhang, *Chem. Mater.*, 2014, **26**, 3104-3112.
- 26 L. Cao, X. Wang, M. J. Meziani, F. Lu, H. Wang, P. G. Luo, Y. Lin, B. A. Harruff, L. M. Veca, D. Murray, S. Y. Xie and Y. P. Sun, *J. Am. Chem. Soc.*, 2007, **129**, 11318-11319.
- 27 G. von Freymann, V. Kitaev, B. V. Lotsch and G. A. Ozin, *Chem. Soc. rev.*, 2013, **42**, 2528-2554.
- 28 X. Guo, C. F. Wang, Z. Y. Yu, L. Chen and S. Chen, *Chem. Commun.*, 2012, **48**, 2692-2694.

Metal ions doped carbon dots with strongly yellow photoluminescence

Jian Cheng, Cai-Feng Wang, Yan Zhang, Shengyang Yang, Su Chen*



Strongly yellow photoluminescent zinc ions doped carbon dots (QY= 51.2%) and their various types of applications were created.